LHC Project Note 101

August 8, 1997
Nuria.Catalan.Lasheras@cern.ch

LHC betatron collimation and non linear effects at injection

N.Catalan Lasheras, J.B. Jeanneret /SL-AP

Keywords: Collimation, Aperture, Non-linear motion

Summary

The collimation system for LHC is designed to clean particles with total transverse amplitude larger than 6σ. Recent results for versions 4 and 5 [1], showed a significant amplitude smear for particles well inside the dynamic aperture. Even if it does not represent a problem for long term dynamic aperture, it may modify significantly the efficiency of the collimation system relatively to a linear model of the ring. In this note we study the implications of amplitude smearing on the collimation efficiency and set an effective geometrical aperture for a given primary aperture.

1 Introduction.

Up to now, the collimation scheme of LHC has been almost entirely studied by using linear uncoupled motion for the primary and secondary protons. The ultimate tracking tool that would combine true scattering in collimator jaws (K2) with the non-linear motion in the machine (SIXTRACK, MAD, DIMAD) does not exist yet. It would be a large programming task to merge the two kinds of software. To evaluate the potential effect of non-linear motion on collimation efficiency, we had a close look at short term tracking data in an amplitude range corresponding to 6-15 r.m.s beam sizes using SIXTRACK [2].

In section 2 we describe the machine parameters used for this study while in section 3 we focus on the effect of the a_3 coefficient on collimation. Based on this first result, we launched another tracking run (section 4) and analysed two main items with the new data.

- Effective primary aperture reduction associated to amplitude smearing (Section 5).
- Collimation efficiency associated to turn by turn amplitude growth at large emittance. In view of these results, we evaluate the potential quench threat by combining the tracking results with realistic evaluations of halo density.(Section 6).

Finally, we summarise in section 7 how each of the above mentioned points will affect the design of the cleaning system.

2 Tracking Parameters

To appreciate the effect of smearing on the collimation, we have tracked and analysed the evolution of particles within the amplitude range in which the collimators will operate.

For the present studies we have used the thin lens version 4 of the LHC lattice with the error distribution with order ≥ 3 of table 9607 [3](no linear coupling). We took the complete set of 60 machines used for dynamic aperture studies [1], and performed six dimensional tracking using SIXTRACK. The momentum deviation was set to 75% of the bucket size that is $dp/p = 0.75 \cdot 10^{-3}$. All runs were made at injection energy. To simplify the input as well as the analysis, we take equal beta values in both axis at the initial point. In a first stage, we tracked particles during 10^5 turns with initial combined amplitude

$$A_{r0}^2 = (A_{0I})^2 + (A_{0II})^2 \text{ in the range } A_{r0} = 6, 7, .., 11\sigma$$

where I and II correspond to the two transverse eigenmodes of the motion. We also used five different values for the initial amplitude ratio in the transverse plane.

$$\tan\theta = \sqrt{\epsilon_{II}/\epsilon_I} \sim A_{II}/A_1 \text{ in the range } \theta = 15, 30, .., 75°.$$

We did again the same tracking on the sixty machines without a_3^{syst} component to verify the preliminary observation that this error was the major contribution to the smearing. This first study and its conclusions are presented in section 3.

For disk space occupancy considerations, proton coordinates can only be recorded every hundred turns. This is a time scale larger than the average number of turns between the first interaction with the primary collimator and its absorption by, usually, a secondary collimator. We therefore tracked again over a shorter time (10^3 turns), to allow us to look at the motion turn by turn. In this case, only three different emittance ratios were tracked and larger amplitudes were privileged.

$$A_{r0} = 6, 7, .., 15\sigma$$

$$\theta = 22.5, 45, 67.5°.$$

For considerations that will be explained in the next section, only the machine including a_3^{syst} multipoles was considered in this case. The results of this analysis are reported in sections 5 and 6.

3 Systematic a_3 effect.

The figure 1 shows the two transverse phase space plots for a particle of initial amplitudes $A_{I0} = A_{II0}$. Due to non-linear effects, the trajectory in these planes is no longer a well determined ellipse as it would be in presence of one-dimensional linear motion. It appears what is known as amplitude smearing, that could be an indicator of the non-linearity of the motion as well as of coupling. In practical terms, the presence of smearing means that particles well inside the dynamic aperture region, could reach amplitudes much larger than their average one.

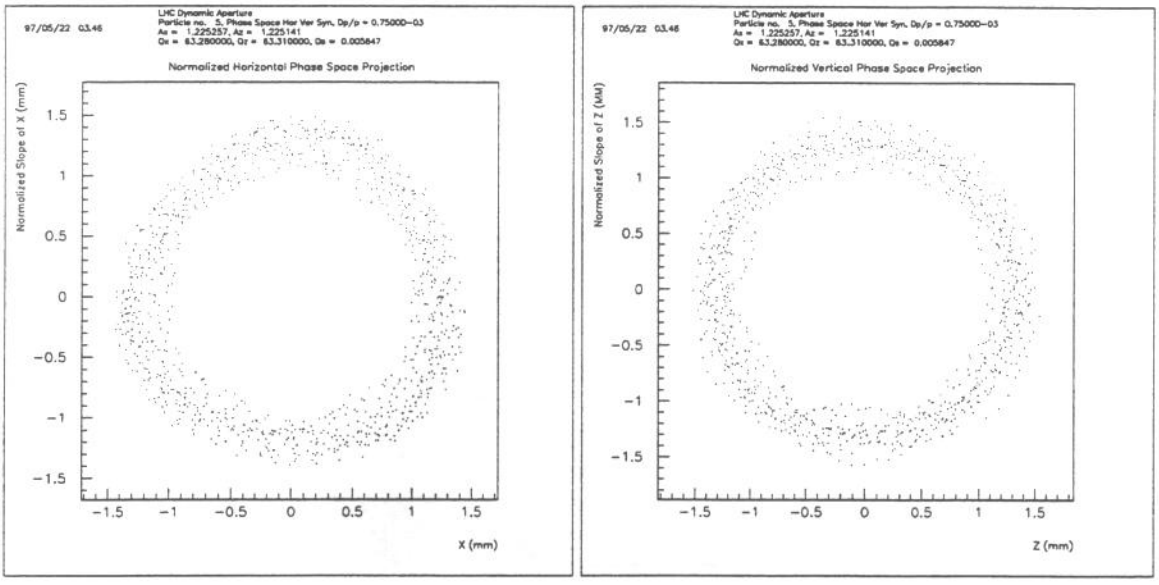

Figure 1: Typical phase space diagram for a particle in the transverse space in the case of non-linearities. In the linear case the trajectory should be a well defined circle in normalised coordinates. The initial amplitude for this particle was 8σ.

We calculate the amplitudes turn by turn at the control point. The smear coefficient is the relative r.m.s. width of the distribution of these amplitudes [4]. It is computed separately for each transverse plane as

$$S_{I/II} = \frac{\sqrt{\langle A_{I/II}^2 \rangle - \langle A_{I/II} \rangle^2}}{\langle A_{I/II} \rangle} \tag{1}$$

and, extended to the combined, or radial amplitude $A_r = \sqrt{A_I^2 + A_{II}^2}$, as

$$S_r = \frac{\sqrt{1/N \sum_{i=1}^{n} (A_{Ii} + A_{IIi} - (\langle A_I \rangle + \langle A_{II} \rangle))^2}}{\langle A_I \rangle + \langle A_{II} \rangle} \tag{2}$$

Values for the smear $S_{I/II} \leq 40\%$ have been found when $A_{0I} = A_{0II}$ whereas for S_r we founded much smaller values ($\approx 10\%$).

That indicated that the one-plane smear is due to non-linear but regular coupling and to some degree, to proper smearing. It was already seen by F. Schmidt [5] that this coupling was mainly due to the systematic a_3 coefficient of the dipoles. Tracking with $a_3^{syst} = 0$ reduced significantly the transverse smear on each independent plane in all cases. The transverse smearing was then comparable to the radial smearing which did not change appreciably, $S_{I/II} \approx S_r \approx 10\%$.

To have a more clever differentiation between true smear and coupling, instead of looking at $S_{I,II}$, we looked at amplitudes in polar coordinates.

$$A_I = A_r \cos\theta$$

$$A_{II} = A_r \sin\theta.$$

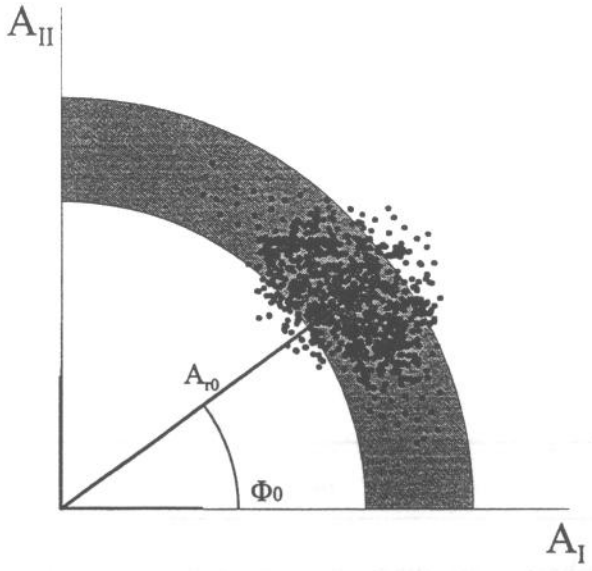

Figure 2: Turn by turn amplitude of a particle. Both the emittance ratio and the radial amplitude change from their initial value. While the coupling tends to fill a ring of radius $\approx A_0$, proper smearing will fill the area around (A_0, θ_0). In the presence of both coupling and smearing a region with a finite radial and angular width is populated. (The figure is an illustration, the real tracking data showed a much weaker effect.)

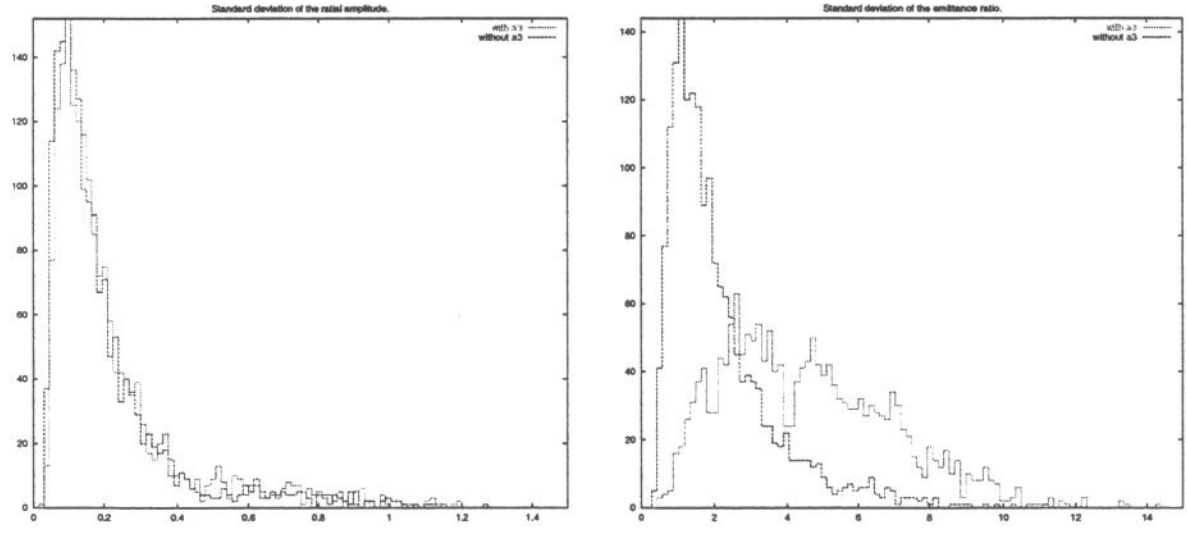

Figure 3: Distribution of the standard deviation for (left) the radial amplitude $\sigma(A_r)$ in sigma units, and (right) emittance ratio $\sigma(\theta)$ in degrees. Both histograms include the 60 seeds, 5 emittance ratios and 5 different values of sigma. The r.m.s. value of a uniform distribution in θ would be $\sigma(\theta) = 26°$. Even with $a_3^{syst} = 0.3 \cdot 10^{-4}$ the coupling time is much larger than our 10^5 turns.

As illustrated in figure 2, the smearing causes both θ and A_r to oscillate around their initial values. The presence of coupling can modify θ by changing drastically both A_I and A_{II} and fill the annular surface of figure 2 without increasing A_r appreciably [1].

We tracked 1800 particles (6 amplitudes, 5 emittance ratios and 60 seeds) 10^5 turns each, once with $a_3^{syst} = 0$ and once again with $a_3^{syst} = 0.3 \cdot 10^{-4}$. For each particle, we computed the variance of $\sigma(A)$ and $\sigma(\theta)$ (equivalent to redefine the smearing) over 10^5 turns sampled every 10^2. The distributions of Figure 3 are made separately for $a_3^{syst} = 0$ and $a_3^{syst} \neq 0$. Obviously, $\sigma(A)$ does not visibly differ in both cases, while a clear additional smearing appears in the $\sigma(\theta)$ distribution for $a_3^{syst} \neq 0$. These figures confirm that coupling is due to the systematic sextupolar error component.

As collimation will do a cut on radial amplitudes A_r [6], we conclude that we can operate with a weakly coupled machine without losing aperture, or altering the efficiency of collimation. As far as collimation is concerned, only radial amplitude changes are important. We can therefore restrict further analysis to the case $a_3^{syst} \neq 0$, closer to the real machine.

Further conclusions on the coupling effects will be discussed in section 7.1.

4 Short term tracking.

As different emittance ratios did not show significant differences in the former section, we tracked again all sixty machines with only three emittance ratios ($\theta = 22.5, 45, 67.5°$) whereas the combined initial amplitude range was extended between 6 and 15 σ.

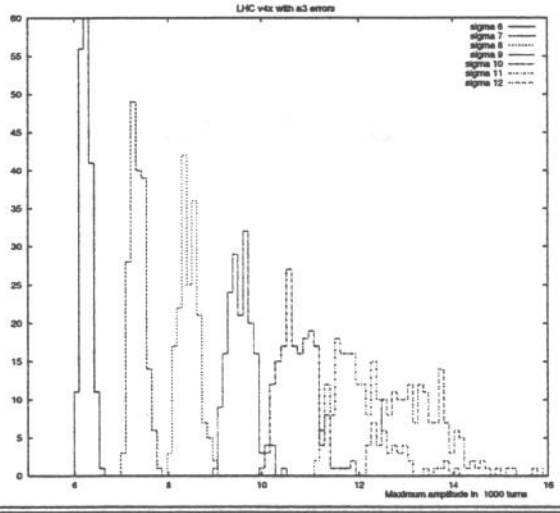

A_{r0}	6	7	8	9	10	11	12	13	14	15
A_{max}	6.60	7.84	9.06	10.41	11.87	18.14	25.25	26.80	35.01	48.71

Figure 4: Maximum combined amplitude on 10^3 turns (r.m.s. beam units). We present 7 different histograms depending on the initial amplitude. From $A_{r0} = 9$ the individual histograms overlap. The left limit coincide with the initial amplitude. The upper limits for all amplitude range are presented in the table.

[1] Provided that coupling is not strong enough to excite resonances. This case was not seen with our data.

In figure 4 we plot the maximum radial amplitude ever reached by a particle during thousand turns. We did one histogram for each initial amplitude.

We can see that for small initial amplitudes, the largest excursions away from the initial value remain small. For larger amplitudes the particle can reach up to 27σ before being lost as in the case of $A_{r0} = 15$ [2]. Secondary particles escaping the collimation system with amplitudes above 11σ could be lost before closing the next turn (see next section).

Not only is it important for us to record the maximum amplitude reached by a particle but also to know if this value is time dependent. If the particle drifts outwards at significant velocity, the maximum amplitude will grow with the number of turns. The absence of drift means amplitude beating without an increase of the equilibrium amplitude. This last case can play an important role in collimation where substantial differences in amplitude can occur since the very first turns after injection.

We drew the same figures reducing the number of turns to hundred and fifty turns. They were not appreciably different. The smearing appears from the first turns and changes very slowly with time. In what follows, the results will always refer to the thousand turns analysis.

As a consequence of the above, we face two major problems.

- When cutting at a certain amplitude with the collimator, some particles with smaller average amplitude will also be eliminated.
- A particle can have a relatively small amplitude at the collimation sections and escape the jaws, but hit somewhere else in the machine if its amplitude increases quickly enough. We have then to determine the biggest excursion a particle can make in one turn.

5 Effective aperture at primary collimators

On the figure 5 we plot the largest excursion in amplitude over 10^3 turns for every initial amplitude A_0, as deduced from figure 4. Up to 10-11σ, the motion is nearly regular and we can fit the data with a linear function.

With a primary collimator at the nominal depth $n_1 = 6\sigma$, a part of the halo will be cleaned down to $n_1^{eff} = 5.59\sigma$. Inversely, to clean only particles with an amplitude larger than six sigma we should put the primary aperture at $\approx 6.53\sigma$.

In the first case we could clean part of the stable core of the beam. In the last one, the surviving secondary halo ([7], [8]) would extend also to larger values and might compromise the collimation efficiency. Obviously, the final decision should be a compromise between these two possibilities. In any case we should fix the specification for the ring aperture such as to allow $n_1 = 7.0$ [9]. The final nominal aperture will depend on the non-linear errors of the definitive LHC machine and its subsequent smearing.

[2] For large amplitude values, the magnetic field model is no longer correct. A more accurate study will require a redefinition of the field errors for radii above the present reference ($\Delta B/B$ for $r > R_r = 1cm$). Non-linearities will surely be stronger. Nevertheless we will perform the complete analysis under the defined conditions.

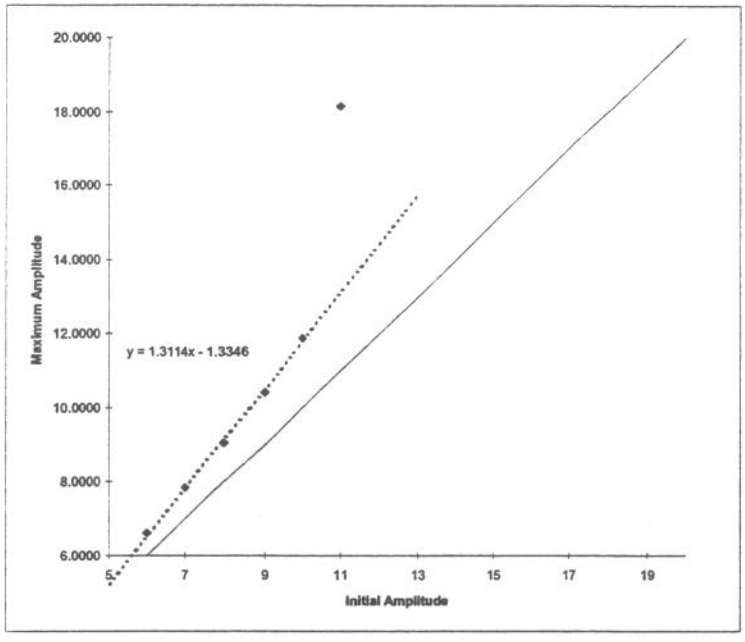

Figure 5: The maximum amplitude reached as a function of the initial amplitude A_0. The primary collimator aperture defines a smaller effective aperture for the beam, in the ratio A_0/A_{rmax}.

Estimator for dynamic aperture

It can be deduced from Figure 5 that the motion is quite regular up to $A_0 \sim 10$. At $A_0 = 11$ the maximum amplitude reached in 1000 turns is already $A_{max} \sim 20$. A change of regime seems to appear around $A = 10.5$ for bad seeds. For the same bad seeds, the dynamic aperture is $d_{10^5} = 9.5\sigma$ [10]. A correlation study between the kink of Figure 5 and d_{10^5} for every seed might help to build another fast estimator for the dynamic aperture.

6 Collimation efficiency

6.1 Single turn considerations.

As stated in section 4 there is a risk of losing the particles somewhere in the ring after having passed the collimation system. To evaluate the probability of such events we computed for each particle the amplitude change turn by turn as well as the maximum amplitude step it ever does.

The results are shown on figure 6 for $A_0 = 8\sigma$ and $A_0 = 14\sigma$. The distribution is crudely Gaussian-like with an average value different from zero (this indicates that particles are very slowly drifting towards bigger amplitudes). In the stable A_0 range (6 to 10 σ), the maximum step is less than 1.0σ in all cases. From these data we can extract the probability that a particle gets a given amplitude step in one turn because of non-linear motion.

Another mechanism which increases substantially the amplitude of a particle is the collimation itself. Via the scattering on primary or secondary jaws a small quantity of particles can be kicked to large amplitudes without being absorbed. This cannot be computed with

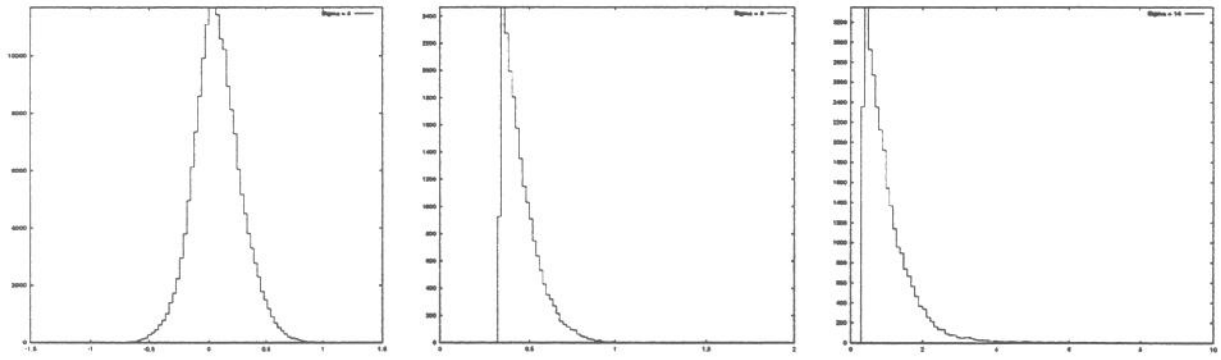

Figure 6: Turn by turn amplitude steps (in σ units) On the left plot all steps are represented for an initial amplitude of $A_r = 8\sigma$. In the centre we have only kept the steps bigger than 0.3σ to see the queue in detail (also $A_r = 8\sigma$). On the right, the case with initial amplitude $A_0 = 14\sigma$ where the increase of amplitude in one turn becomes important (note the change of scale).

SIXTRACK and has to be simulated separately. The studies of collimation efficiency give the distribution of amplitudes of the secondary halo showed in figure 7 as computed with the K2 program.[11].

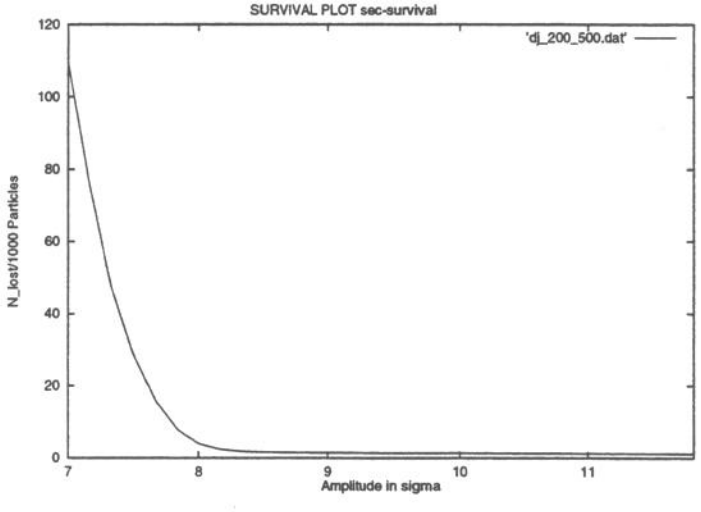

Figure 7: Secondary halo distribution. Number of protons out of 10^5(normalised to 10^3) with amplitude larger than a certain value. Figure obtained with K2 for version 5.0 of the LHC collimation insertion [11].

If the collimators are in working position there are no primary protons at amplitudes larger than the primary aperture ($n_1 = 6\sigma$). Only the particles belonging to the secondary halo have larger amplitudes and are thus susceptible to have an important amplitude increase due to the smearing.

We can therefore take the secondary halo distribution given by K2 as initial conditions to which we apply non-linear tracking.

6.2 One turn losses.

To evaluate the correction in efficiency due to amplitude smearing, we have to somehow connect the probability of losses with the amplitude of the particle. We plot the number of surviving turns versus the maximum amplitude ever reached by the particle either in this thousand turns, or in a shorter time depending on when it gets lost. We can see this plot, obtained from tracking data, in figure 8.

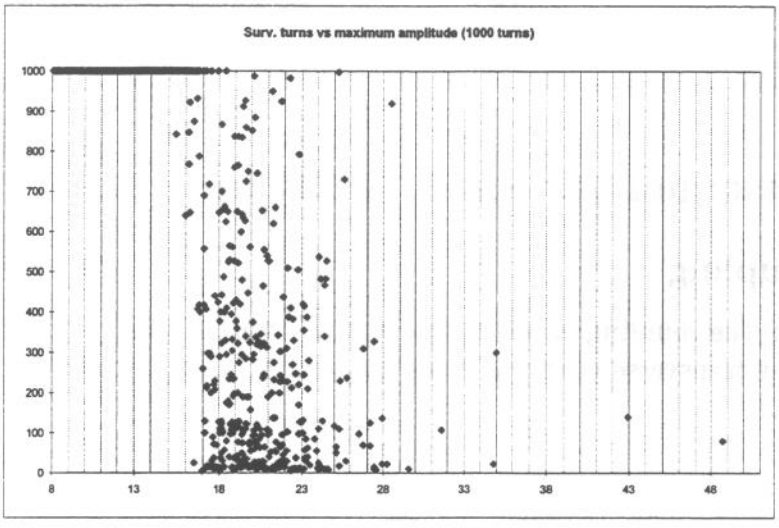

Figure 8: Tracking results. The abscissa is the maximum amplitude reached by a particle over its lifetime on sigma units (1000 turns being the tracking limit). In ordinate the number of turns done by the particles. All initial amplitudes, emittance ratios and seeds are plotted. One net result is that a particle which did not reach 16σ of amplitude is not lost after 1000 turns.

We see that particles get lost only after reaching a radial amplitude $A_r \geq 16\sigma$. We will take $A_{crit} = 16\sigma$ as a sort of short-term dynamic aperture.

Particles at large amplitudes that do not get lost in the physical aperture of the machine, will do at least one more turn and will then be absorbed (with nearly 100% probability) by the cleaning section. Thus, we only have to care for a sudden increase of amplitude in a time shorter than the machine revolution time. We calculate the probability to reach this critical amplitude A_{crit} in one turn as follows

$$P(16) = P_c(16) + P_c(15)P_{15}(1) + P_c(14)P_{14}(2) + P_c(13)P_{13}(3) + P_c(12)P_{12}(4)\cdots \quad (3)$$

$P_c(N)$ is the probability of having a proton scattered by the jaws to an amplitude of N sigma (obtained via K2).

$P_N(M)$ is the probability a proton with an average amplitude of N sigma makes a step of M sigma in one turn due to non-linear motion deduced from tracking data (figure 6). In our particular case $M = 16 - N$.

For amplitudes $N \leq 12\sigma$ the maximum step per turn is never larger than $\approx 3\sigma$ so the probability of reaching a radial amplitude of 16σ $P_N(16 - N)$ is always zero for $N \leq 12$.

Applying the data obtained with K2 and SIXTRACK we obtain

$$P(16) = 1.2 \cdot 10^{-3}.$$

The series (3) converges rapidly the second term on the series being already very small $(1 \cdot 10^{-5})$. The dominant term which will determine the peak losses in the machine will be then the radial profile of the escaping scattered protons.

Non linear motion can modify this profile as well as the phase distribution and thus the linear approximation used to compute dilution of the losses along the ring could no longer be a precise enough estimator.

7 Consequences for collimation

7.1 Coupling

In Section 3, the coupling effects related to a_3^{syst} were studied. Of course, many other causes may induce a transverse coupling, even temporarily, associated to more or less slowly varying parameters.

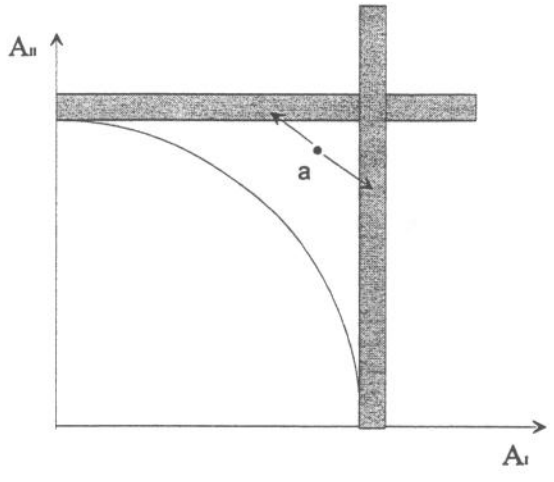

Figure 9: A collimator set-up with only horizontal and vertical jaws.

Let us suppose the cleaning system is made of horizontal and vertical collimators only. In the absence of coupling a proton might be located near the upper right corner in the amplitude plot of figure 9. Would a coupling mode appear, the stored protons would touch one of the collimators after a certain time that we can call the coupling time. All the protons lying between the circle and the square of the figure, as delimited by the jaws would be lost during that coupling time. This kind of instability might be dangerous by inducing strong transient proton losses.

For geometrical aperture considerations, a circular collimator setting is needed [6]. We are confirmed in this choice by the argument of coupling discussed here.

7.2 Smearing and primary aperture

It is shown in Section 5 that with primary jaws set at $n_1 = 6$, the effective aperture is $n_1^{eff} = 5.56$. The reduction of $\sim 7\%$ is well inside the margin given by the specification for geometrical aperture, set to $n_1 = 7$, the minimal need being $n_1 = 5.5$.

We can apply this linear approximation up to $10 - 11\sigma$. Cleaning with a primary collimators aperture of $n_1 = 10\sigma$ will imply $n_1^{eff} = 8.64\sigma$. This aperture can compare with the final one where the collimators will be close to the dynamic aperture. The effects of non-linearities will be those of a stable region border. Applying the reduction on effective aperture due to non-linear effects corresponding to the present dynamic aperture ($\sim 14\%$), we will obtain a value for $n_1 = 5.2$.

A simple rescaling of the primary aperture is probably not accurate enough. A more elaborated study of the mechanisms which define the Dynamic Aperture as well as of the real magnetic multipoles at large amplitudes is necessary.

7.3 Large amplitudes and collimation efficiency

We have seen that as far as quick absorption is assured, the correction of peak losses as a consequence of non-linear motion is quite negligible. Efficiency studies currently under way, will confirm whether the absorption of the secondary halo protons is quick enough to neglect the slow amplitude increase caused by non-linearities.

Nevertheless, the way these losses are going to be distributed in the machine depend on the dilution of the secondary halo and could be modified in case of non-linearities. A dedicated step-tracking with aperture control at least at the end of each element is necessary to evaluate how the linear and non-linear efficiency differ.

Acknowledgements

The authors would like to thank M.Böge for his help with the SIXTRACK tracking code and the post-processing of the data. For the same reason, and for the benefit of fruitful discussions, we specially thank F. Schmidt.

References

[1] M. Böge, F. Schmidt. Tracking studies for the LHC optics version 4 at injection energy. LHC Project Report 103.

[2] F. Schmidt. SIXTRACK. User's reference Manual, CERN/SL/94-56(AP).

[3] Working group on field component. L. Walkiers et al. 26/6/96.

[4] M.A. Furman and S.G. Peggs. A standard for the smear. SSC-N-634.

[5] F. Schmidt. LHC Machine Advisory Committee meeting No 4. June 1997.

[6] Thomas Trenkler and J.B. Jeanneret. The principles of two stage betatron and momentum collimation in circular accelerators. SL/95-03(AP) LHC-Note 312.

[7] D.I. Kaltchev, M.K.Craddock, R.V.Servranck, J.B.Jeanneret. PAC96, Sitges, May 1996, and LHC Project Report 37, July 1996.

[8] D.I. Kaltchev, M.K.Craddock, R.V.Servranck, J.B.Jeanneret. PAC97, Vancouver, May 1997, proc. to appear and LHC Project Report, to appear.

[9] J.B. Jeanneret and Thys Risselada. LHC Project Note 66, September 1996.

[10] M.Böge et al. LHC Project Report 106, July 1997.

[11] N.Catalan Lasheras, J.B. Jeanneret, D. Kaltchev, T. Risselada. Note to appear.